Exploring isovist fields: space and shape in architectural and urban morphology

Michael Batty
Centre for Advanced Spatial Analysis (CASA), University College London, 1 – 19 Torrington Place, London WC1E 6BT, England; e-mail: mbatty@geog.ucl.ac.uk
Received 23 March 2000; in revised form 18 September 2000

Abstract. The space that can be seen from any vantage point is called an isovist and the set of such spaces forms a visual field whose extent defines different isovist fields based on different geometric properties. I suggest that our perceptions of moving within such fields might be related to these geometric properties. I begin with a formal representation of isovists and their fields, introducing simple geometric measures based on distance, area, perimeter, compactness, and convexity. I suggest a feasible computational scheme for measuring such fields, and illustrate how we can visualize their spatial and statistical properties by using maps and frequency distributions. I argue that the classification of fields based on these measures must be a prerequisite to the proper analysis of architectural and urban morphologies. To this end, I present two hypothetical examples based on simple geometries and three real examples based on London's Tate Gallery, Regent Street, and the centre of the English town of Wolverhampton. Although such morphologies can often be understood in terms of basic geometrical elements such as corridors, streets, rooms, and squares, isovist analysis suggests that visual fields have their own form which results from the interaction of geometry and movement. To illustrate how such analysis can be used, I outline methods of partitioning space, covering it with a small number of relatively independent isovists, and perceiving space by recording properties of the isovist fields associated with paths through that space.

1 Definitions and approaches: isovists and fields

Benedikt (1979) describes an isovist as "the set of all points visible from a given vantage point in space" (page 47). An isovist thus defines a field of vision from which various geometrical properties, such as area and perimeter, can be calculated. Isovists can be defined for every vantage point constituting an environment, and the spatial union of any particular geometrical property defines a particular isovist field. However, the only work that has sought to extend these ideas has concentrated on the shape of isovists within their fields. Space is described, for example, by Hillier and Hanson (1984), as a set of axial lines which in turn are defined as those longest lines of sight spanning an environment partitioned into disjoint convex spaces. Convex spaces can be directly associated with isovists but this theory of space syntax defines away any measure of Euclidean space which isovists enable, in favor of relational analysis based on non-planar graphs. More recently, Peponis et al (1997) have developed various measures for partitioning space within buildings into convex sets, producing what they call 'e-partitions': visually stable sets of convex spaces which cover any plan. The lines and spaces which characterize such partitions (e-lines and e-spaces) are clearly related to both axial lines and isovists, although formal relations have not been developed.

A theory of space based on convex partitions assumes that space can be uniquely broken into convex and nonconvex sets which meet some criteria of minimality in number. It is far from clear, however, that there will ever be any such general theory (O'Rourke, 1987). Defining axial lines is an ad hoc process, for there is no formal proof that a space can be divided into a unique set of convex spaces represented by the "the least set of fattest spaces" which can thence be spanned by "the least set of such straight lines" (Hillier and Hanson, 1984, page 92). Even if there were, there is then controversy about the relative importance of one vista (axial line) versus another, especially when

criteria other than Euclidean distance are used in their definition. Hence, we conjecture that there is no formal relation between axial lines and isovists.

Peponis et al (1998a; 1998b) have extended the formal analysis of convexity further, but their emphasis is on summarizing space by using some lesser set of spatial units, rather than on working directly with the properties of visual fields. Indeed, they are skeptical about extending Benedikt's (1979) original approach. They say: "Though surfaces can be described completely according to the positions of edges and corners, which are always a finite set, isovists can never be drawn from all possible points. One implication of this is that isovist analysis...cannot readily be automated or proceduralized to deal with an entire plan" (pages 769–770). In this paper, I will show that their skepticism is unwarranted but, more than this, that a more fruitful approach than that engendered by space syntax can be developed if the focus is shifted back to the Euclidean analysis of visual fields using isovists.

The problem with partitioning space according to its convex properties is that the usual approach involves defining space by using vectors and this presumes a degree of continuity in the description of space which is unrealistic computationally. In fact space is always characterized, to some degree of resolution, with respect to its computation and digital representation (on raster devices) and with early-21st-century computing power, very fine levels of resolution, lower than anything used hitherto in space syntax analysis, are possible. In this paper, I assume that the analysis of space must begin with spatial relations based on some homogeneous and indivisible unit defined on some regular tessellation of the plane, in this case a grid, which can be uniquely and unambiguously mapped onto the pixels of an associated display device. For some problems, Peponis et al (1997) may be correct in their assumption that, "It is always necessary to devise ways for sampling the set of points from which we will draw the isovist..." (page 770), but in the examples I develop here, the number of units defining each isovist and field is sufficient to allow descriptions, computations, analysis, and display which are not prone to unacceptable measurement errors.

This approach is complementary to that being developed by Turner et al (2001). They too develop isovist analysis on a regular tessellation in which each unit is associated with a geometric point (grid centroid), but their emphasis is on using these points to define visibility graphs and thence to use these visibility graphs to represent convex spaces. Convexity, I will argue, is not the most significant issue in defining space, nor indeed is relational analysis built upon it, and my analysis will thus follow more directly in the tradition that was begun by Benedikt (1979). Ratti and Richens (forthcoming) also define isovists and isovist fields by using image processing methods where their emphasis is on the geometry of the field and ways of moving within it; like Turner et al (2001) and myself, they adopt a regular grid as the medium on which all subsequent analysis is developed.

Before I develop my formal and empirical analysis, I must provide a wider motivation for this approach. By defining visual fields, I am able to pose and to answer certain basic questions of relevance to architects and urban designers, and of relevance, I hope, to good architecture. These questions revolve around issues concerning what we can see from different vantage points. 'How far can we see, and how much can we see?' are key issues in developing good design, and an appropriate theory of space should be able to provide unequivocal answers to these questions. Properties derived from such measures such as 'how much' space is enclosed, and what obstacles interfere with 'how far' and 'how much' one can see, are also relevant. These emphasize convexity and compactness and thus relate to space syntax, although here, I will not concentrate on convexity per se. Once we have such procedures for generating isovist fields and rapid computation of their statistics, we are in a position to develop many

possible analyses. I will begin with a preliminary classification of isovist fields for different building complexes, and, although I examine only a handful of examples here, these are enough to show that a sustained attack on the classification of such spatial structures is a prior essential to any subsequent science.

I first represent the problem formally and introduce the various statistics associated with each isovist which together define different types of isovist field. I will focus on measures of distance, area, and compactness, illustrating the basic ideas for two simple geometries characteristic of a building and a street scene. I then apply the analysis to three distinct building and city types in England: the Tate Gallery main building, lower Regent Street and Piccadilly Circus, and the town centre of Wolverhampton. These examples show differences between fields based on rooms in buildings and those based on streets and squares constituting towns. To demonstrate how these methods can be used to enhance our cognitive and spatial understanding, I illustrate how we can partition space based on a ranking of isovists according to their relative accessibility in the Tate Gallery, and then show the kind of visual experience associated with a typical 'walk' through the Regent Street area. I conclude with ideas for further research.

2 Representing isovists
2.1 Neighborhoods and clustering
An isovist is defined as a set of points or vertices of a graph, $j \in Z_i, j = 1, 2, ..., n_i$, where Z_i is the generic field associated with the vantage point or vertex i, and n_i is the total number of points in Z_i, including the vantage vertex i. Vertices are associated with the regular units into which space is divided, and for each unit I define a geometric point—a centroid—which roots the vantage point at the origin of the isovist. I illustrate these, and subsequent definitions for a typical tessellation based on a regular grid, in figure 1 (see over); this shows the original form of an isovist as a polygon (Benedikt, 1979) [figure 1(a)], the regular subdivision of space from which the polygon is approximated [figure 1(b)], the units within the polygon which define the vertices of the isovist's visibility graph [figure 1(c)], and the way the perimeter of the polygon is defined from a subset of the graph's edges [figure 1(d)].

Z_i is sometimes called the neighborhood of the vertex i (Watts, 1999), whereas the total number of vertices in the entire space—that is, within each isovist field—is defined as n, where $i, j = 1, 2, ..., n$. The average number of vertices in each isovist or neighborhood is $\bar{n} = \sum_i n_i / n$, where it is clear that the fields of vision associated with each isovist Z_i can overlap. A workable definition of the field treats each isovist as part of a visibility graph $\{A_{ij}\}$ where:

$$A_{ij} = \begin{cases} 1, & j \in Z_i, \\ 0, & \text{otherwise}, \end{cases} \tag{1}$$

and where there is a distance associated with each edge A_{ij} defined as:

$$d_{ij} = \begin{cases} [(x_i - x_j)^2 + (y_i - y_j)^2]^{1/2}, & \text{if } A_{ij} = 1, \\ \infty, & \text{otherwise}. \end{cases} \tag{2}$$

Associated with each edge $[i, j]$ and its vertices i, j are coordinate pairs $\{x_i, y_i\}$ and $\{x_j, y_j\}$. The graph for which $\{A_{ij}\}$ is the adjacency matrix is symmetric, and thus $A_{ij} = A_{ji}$ or, in matrix terms, $\mathbf{A} = \mathbf{A}^{\mathrm{T}}$. These definitions are illustrated in figures 1(b) and 1(c).

It is now possible to define the neighborhood more clearly as the number of in-degrees or edges emanating from any vantage point i. Then:

$$n_i = \sum_j A_{ij}, \tag{3}$$
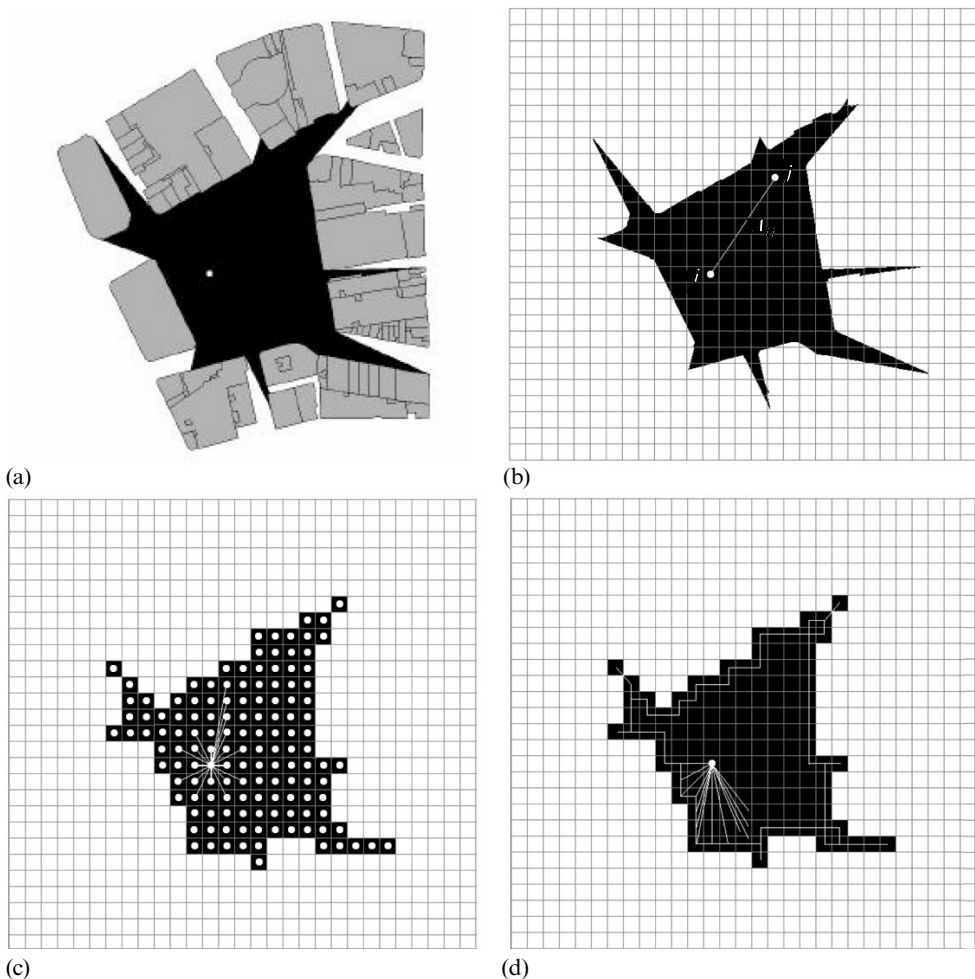
Figure 1. Defining isovists through visibility graphs: (a) the isovist polygon generated from the viewpoint defined by the open circle at 'o'; (b) a typical edge in the visibility graph defined about the root vertex of the isovist at i; (c) the isovist polygon as a set of vertices—grid centroids—and a sample of edges; and (d) the perimeter marked out from rotating the visibility graph edges around the viewpoint 'o', with a sample of edges shown.

from which it is clear that $n_i = n_j = \sum_j A_{ij} = \sum_i A_{ji}$. The total number of degrees or directed edges in the entire space is $N = \sum_i n_i = \sum_j n_j = \sum_{ij} A_{ij}$, which can be used to compute the average number of vertices (or edges) $\bar{n}$ per isovist, as above. It is worth noting that Turner et al (2001) and Watts (1999) define equivalent adjacency relations but without including the self-loop A_{ii}, that is, by setting $A_{ii} = 0, \forall i$. Furthermore, the visibility graph defined from $\{A_{ij}\}$ is usually treated as nondirected, although it is more straightforward if it is considered to be directed but symmetric with respect to computations using the matrix $\mathbf{A}$. Edges (or arcs) in the graph-theoretic sense should not be confused with edges as geometric lines which define spaces as polygons, as used by Peponis et al (1998a; 1998b) in related work.

This graph-theoretic interpretation greatly facilitates the analysis of isovist fields in terms of their shape, that is, the convexity of individual isovists. If all the points or vertices n_i within any isovist Z_i are connected to one another, that is, if each vertex j has an identical overlap with every other vertex in terms of its own isovist, then there

are a total of n_i^2 directed edges in the set. Conventional indices of clustering are based on comparing the actual number of edges in any isovist Z_i, called $E(Z_i)$, with this theoretical maximum. The cluster index for each set i is thus defined as

$$\gamma_i = \frac{E(Z_i)}{n_i^2}, \tag{4}$$

whereas an average cluster index γ for the entire system is a simple average of the individual indices in equation (4), that is:

$$\gamma = \frac{\sum_i \gamma_i}{n}. \tag{5}$$

To determine the number of nondirected links between vertices in Z_i, we need to compute all paths of length 2 in the graph, determine which of these form part of the isovist Z_i, and use these for $E(Z_i)$ in equation (4). A form for this is given as

$$\gamma_i = \frac{\sum_j A_{ij} \sum_k A_{ik} A_{kj}}{\left(\sum_j A_{ij} \right)^2}. \tag{6}$$

As Turner et al (2001) show, this is a measure of convexity, in that, as $\gamma_i \to 1$, the visibility graph associated with Z_i converges to a completely connected graph. With the definition that its vertices form part of a regular tessellation of the plane, this implies that the space it describes is convex.

A related measure used by Turner et al (2001) is based on the shortest path length between any two vertices defined from the relational matrix $\{A_{ij}\}$. The shortest path between any two vertices is given as L_{ij}, whereas the average shortest path associated with an isovist Z_i is $L_i = \sum_j L_{ij}/n_i$. Shortest paths can be defined by using an algorithm which seeks to find the least power of the adjacency matrix at which a path exists between any two vertices i and j (Buckley and Harary, 1990). By defining the matrix $\mathbf{A}_{ij}^m$ as $\sum_k A_{ik} A_{kj}^{m-1}$, the length of the shortest path is given as

$$L_{ij} = m, \quad \text{if} \quad \mathbf{A}_{ij}^m > 0 \quad \text{and} \quad \mathbf{A}_{ij}^{m-1} = 0. \tag{7}$$

As no path in a connected graph can be longer than n links, equation (7) ensures that the path matrix $\mathbf{L}_{ij} > 0$, $\forall ij$, when $m = n$. The average path length for the entire system is then calculated as $L = \sum_i L_i/n$. These same measures have been used extensively by Watts and Strogatz (1998) and Watts (1999) to define systems called 'small worlds'. Small worlds are graphs characterized by a high degree of clustering $\gamma \gg 0$, and a small path length $L \ll n$, and there is some suggestion that systems of the kind that define spaces in cities must be small worlds if they are to exhibit the requisite complexity engendered by normal social and spatial relations. Turner et al (2001) have laid the ground-work for demonstrations of how isovist analysis can be linked to small world theory.

2.2 Distance and area
In his initial analysis of isovists, Benedikt (1979) identified six geometric measures from which isovist fields could be established: area; perimeter; occlusivity (or length of occluding boundaries within the isovist); variance and skewness of the radial distances around each vantage point; and a measure of compactness called circularity, defined as the ratio of the square of the perimeter to area (Davis and Benedikt, 1979). Conroy (2000) has extended and modified this set of measures in defining the properties of isovists in virtual space. My measures are similar. I will make a distinction between five

basic measures and two derived measures defined for each isovist. I will develop simple statistics of the spatial distributions of these measures which in turn define the statistical properties of their associated isovist fields. In essence, my analysis, like Benedikt's (1979), lays much emphasis on measures of the Euclidean geometry of the space which, I argue, is a prerequisite to any subsequent analysis of spatial relations.

The first three measures define standard radial distances: the maximum or farthest distance which can be seen from the vantage point i, d_i^{max}; the minimum distance d_i^{min}, and the average distance $\bar{d}_i$ computed as:

$$d_i^{max} = \max_j \{d_{ij}\} ,\tag{8}$$

$$d_i^{min} = \min_j \{d_{ij}\} ,\tag{9}$$

$$\bar{d}_i = \frac{\sum_{j \in Z_i} d_{ij}}{n_i} .\tag{10}$$

These statistics measure 'how far we can see' in three different ways and are closely related to 'how much we can see', best characterized by the area a_i and the perimeter p_i of each isovist. By using the adjacency matrix, area is the number of vertices within the neighborhood. Each point $j \in Z_i$ is associated with a standard area Δ, and thus the area of any isovist can be approximated as

$$a_i \approx \Delta n_i = \Delta \sum_j A_{ij} .\tag{11}$$

In fact, as we work with both points and distance measures defined on a regular grid of fine resolution, the area associated with any isovist can be defined more conventionally as

$$a_i = \int_0^{2\pi} \int_0^{R_m} r(m) \mathrm{d}\theta \mathrm{d}r(m) ,\tag{12}$$

with $r(m)$ the radial distance about i, R_m the bounding radius associated with the radial $r(m)$, and θ the angle of rotation. This can be approximated as

$$a_i \approx \frac{1}{2} \sin\left(\frac{2\pi}{M}\right) \sum_{m=1}^M R_m .\tag{13}$$

Equation (13) converges to πR^2 when $R_m = R$ and when $M \to \infty$. It provides the basis for a rotation of rays around the vantage point i to the perimeter of the isovist, as explained by Davis and Benedikt (1979), which is consistent with the method of computation used below. This is implied in figure 1(d). The perimeter is computed directly by rotating the distance from the vantage point to the perimeter, around the circle; each increment of the perimeter is calculated as

$$p_m = \left[(x_m - x_{m-1})^2 + (y_m - y_{m-1})^2\right]^{1/2} ,\tag{14}$$

from which the perimeter is derived as

$$p_i = \sum_{m=1}^M p_m .\tag{15}$$

The five measures—d_i^{max}, d_i^{min}, $\bar{d}_i$, a_i, and p_i—form the basis of five isovist fields which will subsequently be computed in the examples. I will also compute statistics of their distributions such as average distance, area and perimeter, and higher order moments such as variance and skewness. Before I do so, I must introduce a second set of measures which throws some light on the various shapes which such isovists exhibit.

2.3 Measures of shape: compactness and convexity

I have already suggested that useful measures of shape for isovists and their fields are the cluster indices defined in equations (4) and (5) which detect the degree of convexity of isovists. These, however, do not account for variations in compactness. For example, long thin shapes—streets—can have the same degree of convexity as short fat spaces—urban squares. Measures of compactness as well as convexity per se are required in the measurement of isovist fields, and these can easily be generated from the distance, area, and perimeter measures defined so far.

The first measure of compactness, Γ_i, is defined as the ratio of average to farthest (or maximum) distance from each vantage point:

$$\Gamma_i = \frac{\bar{d}_i}{d_i^{\max}}. \tag{16}$$

If, for example, the isovist is a circle with i as its centre, then it is clear that the average is the same as the maximum and $\Gamma_i = 1$. In contrast, an isovist which is a straight line originating from one of the end points, has a compactness $\Gamma_i = 0$, owing to the fact that all but one of its radial distances has a value of zero; as the number of these distances tends to infinity, the measure of compactness will tend to zero. The measure thus varies from 0 to 1, with low values for stringy noncompact linear shapes to high values for compact circular shapes.

An alternative measure, Ψ_i, originates from area and perimeter, and is defined as the ratio of the radius of an idealized circle associated with the actual area of the isovist to the radius of an idealized perimeter from the actual perimeter in question. Then

$$\Psi_i = \left(\frac{a_i}{\pi}\right)^{1/2} \bigg/ \frac{p_i}{2\pi}, \tag{17}$$

which, like equation (16), varies from a value of 0 for a straight line isovist with the vantage point at one of its ends to 1 for a circle with its vantage point at its centre. This measure falls within $0 \leqslant \Psi_i \leqslant 1$ which I state without proof. As I will suggest below, this measure also appears to covary with the convexity of the space.

These measures are both normalized to a linear form, in that Γ_i is based on one-dimensional (1D) radial distances, whereas Ψ_i is based on linear measures normalized from a two-dimensional (2D) area and a 1D perimeter. These measures are simply sharpened if their values are squared, that is, by computing Γ_i^2 and Ψ_i^2. Other measures, such as those based on ratios of minimum to maximum and average distances, have been tried, although in all experiments to date, the minimum distance measure is much less of a discriminator of shape and size than the average or the maximum. I will thus use Γ_i and Ψ_i in the analysis which follows although I have not yet been successful in finding an exact index for detecting convexity, other than that introduced by Turner et al (2001) based on clusters within visibility graphs.

3 The distribution of shape: isovist fields for simple geometries

3.1 Agent-based computation

Peponis et al's (1997) reservations about computing isovist fields at a sufficiently fine level of resolution in a sufficiently manageable time are being resolved through developments in conventional computation. Rapid increases in speed and memory on the current generation of workstations, as well as new modes of computation that employ parallelism are providing the momentum. To compute isovist fields, I will adopt the latter course, using a widely available software package called 'StarLogo' from the Media Lab at MIT (Resnick, 1994). This is built around the notion that individual

agents or objects can be controlled in any space, usually a 2D grid, through simple commands which affect each and every agent immediately. This simultaneity is based on simulating a parallel architecture which enables very fast processing of thousands of agents. The current generation of software enables grids of up to 250×250 cells to be represented with an upper limit of 16 000 or so agents.

In essence, each isovist field is computed by placing an agent at the given vantage point i and 'walking' that agent in a given direction until the agent encounters an obstacle (Batty and Jiang, 2000). This is akin to walking the agent to the perimeter of the isovist and as the agent walks, various geometric characteristics of the walk are 'remembered'. To detect the entire isovist, the agent then returns to its vantage point and begins another walk at some angular displacement from the previous walk, with the procedure continuing until the agent has walked in every direction around the 'clock' of 2π radians, as implied in figure 1(d). The five basic measures presented in equations (8), (9), (10), (13), and (15) are computed incrementally during these walks. All isovists $i = 1, 2, ..., n$ are computed together as the efficiency of the software depends upon a large number of agents acting in the same way. Once each agent has completed its rotational walk, isovist fields associated with each of the five measures are immediately available.

The precision and the accuracy of these fields depend upon the level of resolution of the system and the number of walks used to define the circular field of vision around each vantage point. For a grid based on $m \times m$ pixels, then, for every grid cell to be detected during the walks, the angular increment from one walk to the next is set as $\Theta \leqslant \arctan(1/m)$. For a system based on 200×200 pixels, this angle must be less than 0.005 radians and thus the number of walks which each agent makes must be not less than $1257 \approx 2\pi/0.005$. A rough idea of the number of computations needed can be provided if the isovist field is simply an unobstructed square grid with periodic boundary conditions and the line of sight is no longer than the maximum distance across the grid, which is $200(2)^{1/2}$. Each walker will walk 283 pixels 1257 times to complete their circular rotation, and with 16 000 agents in the space, this would require over 5691 million basic computations. In current implementations of these algorithms, there are over 70 individually distinct calculations for each vantage point, giving a total of around 4000 billion computations. On a Macintosh G3 (266MHz), this size of problem takes around 2 hours.

A grid of 200×200 pixels with 40 000 cells might be considered small for the kinds of physical problems that I intend to deal with, although an acceptable size of grid square for the Tate Gallery example of around 1 m^2 can easily be handled using this software. This seems to be close enough to the sight lines that would detect appropriate detail in geometric shapes within such a complex. For city centres and street scenes, the levels of resolution which this software allows is too coarse to pick up fine detail but the results will be considered to be sufficiently reliable to aid interpretation.

However, other modes of computation are being developed by Turner et al (2001) who take a more conventional approach and are able to deal with bigger grids, but with a marked increase in computation time. Ratti and Richens (forthcoming) also suggest fast techniques of computation based on image processing. Thus, I do not consider the computation problem an issue any longer for isovist fields. The display problem also depends on appropriate software. However the StarLogo package has highly developed capabilities in this regard and if isovist fields based on contour maps are required, as originally suggested by Benedikt (1979), then it is easy to export fields of pixels to appropriate packages based on desktop GIS, such as 'ArcView'.

### 3.2 The simplest geometry: the T-shape within a square

Before I develop the simplest example, it should be noted that the five basic measures and the two shape statistics define seven isovist fields that can be represented in several ways. I will present these as greyscale pixel maps with the largest values the lightest on each scale. I will not display these as contour maps for it is easy enough to visualize these surfaces from the pixel maps but I will examine the distribution of the pixel values for each field by using conventional statistical measures. I will graph the actual distribution of isovist values. Spatial morphologies of the kind that are being dealt with, which often combine long thin spaces with short fat ones, tend to be rather different from the 'normal distributions' which dominate statistical theory. I will also compute a variety of other measures based on moments around the mean, namely the mean itself (or first moment), the standard deviation which is the square root of the variance (the second moment), and the skewness coefficient (the third moment).

The T-shape is the test example used by Turner et al (2001) for which there are exact published comparisons. This is a solid T-shaped block occupying 561 grid squares centred in a 51×51 grid, leaving 1840 vantage points used to define the isovist fields. The square is bounded by another solid object which is one pixel in width and takes up some 200 grid squares. This serves to contain all the isovists to within the square grid. The edge effects introduced by this bounding will be noted below. The shape is shown in figure 2 and it is immediately obvious that there are no very narrow isovists within the field, and that each isovist is 'relatively' compact. The corner points are likely to be of interest in that it is at these points that isovist fields exhibit sharp discontinuities. These are the points at which the visual field changes most radically as new vistas are revealed. The two isovists in figures 2(a) and 2(b) illustrate these differences.

(a)   (b)   (c)
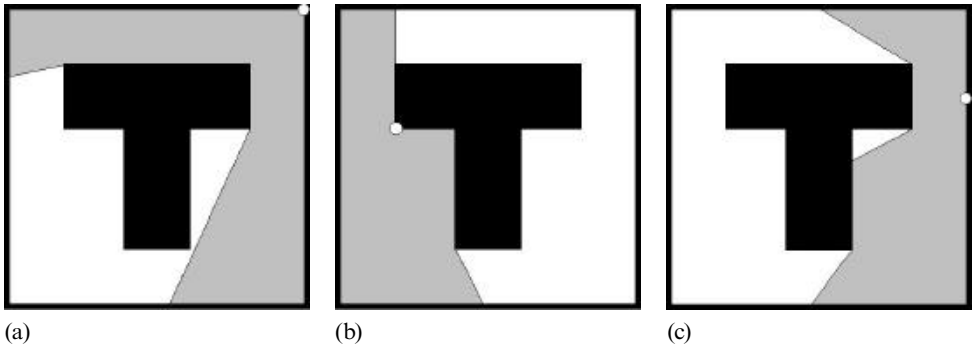
Figure 2. Typical isovists associated with the basic T-shape.

In figure 3 (over), the seven fields are presented. The field of average distance in figure 3(b) is clearly dominated by edge effects, with the largest averages in the 'most open' spaces away from the edges of the T-shape and the bounding box in which it sits. These edge effects are most clearly seen from the plot of minimum distance in figure 3(c) which is correlated with the average distance at around 0.5. In fact, I will not show this minimum distance field in any of the examples below because in systems with many edges, this information does not vary radically enough for it to be of much relevance to substantive interpretations. The maximum distance, however, in figure 3(d) is significant in that this shows the importance of the areas most distant from the T-shape. When the area and perimeter in figures 3(e) and 3(f) are examined and compared with maximum distance, all correlations are greater than 0.84, indicating 'how far' and 'how much' one can see are similar, thus implying a higher degree of compactness than might be expected in street scenes. Note that
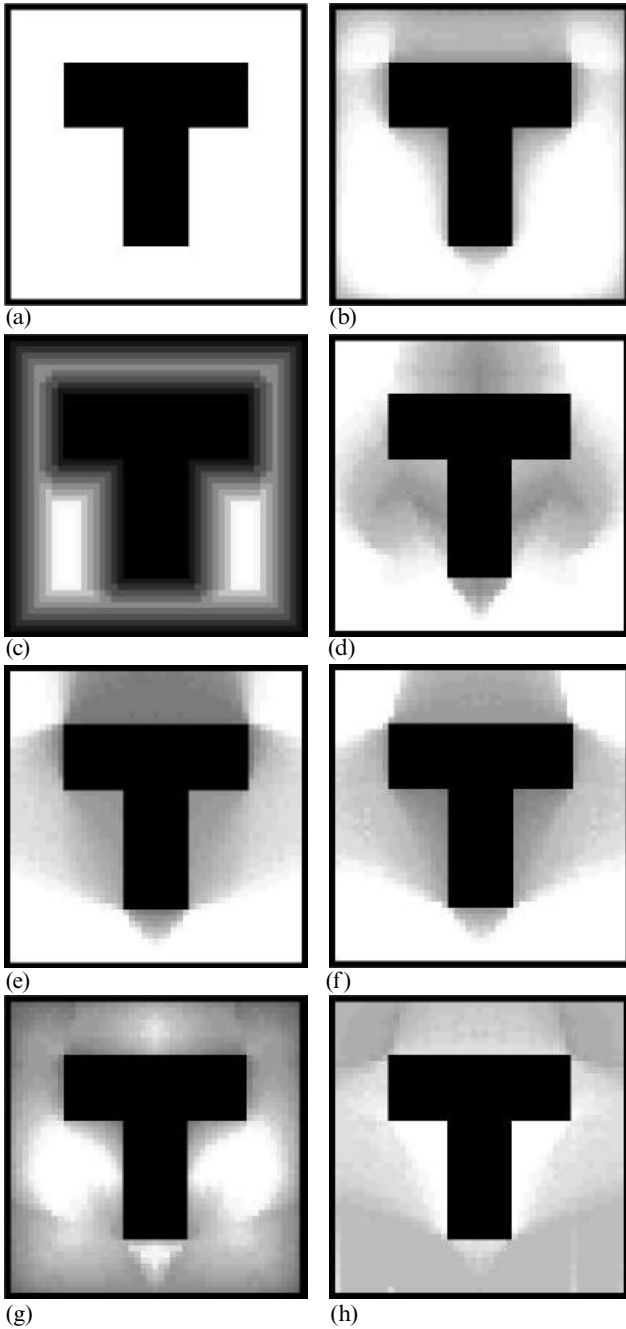
Figure 3. Isovist fields for the T-shape: (a) the basic T-shape; (b) the average distance; (c) the minimum distance; (d) the maximum distance; (e) the area; (f) the perimeter; (g) the compactness ratio; and (h) the cluster ratio.

figure 3(e), the area seen, is identical to figure 4(b) in Turner et al (2001, page 109 of this issue).

The last two fields [figures 3(g) and 3(h) based on $\{\Gamma_i\}$ and $\{\Psi_i\}$, respectively] illustrate features of compactness and convexity. The ratio field $\{\Gamma_i\}$ seems to be the better measure of compactness in that it picks up those areas above, below, and within the interstices of the T-shape as being the most compact. In contrast, the shape measure $\{\Psi_i\}$ tends to ignore the influence of boundary effects and is much closer to the measure of clustering defined in equation (4). This is, in effect, a measure of the proportion of the isovist which can be seen from all points within it, thus a measure of convexity. A comparison of figure 3(h) with figure 5(a) in Turner et al (2001, page 110 of this issue) reveals a close spatial correspondence, but as there is no formal demonstration that the index of shape $\{\Psi_i\}$ and the index of clustering $\{\gamma_i\}$ are similar, this is left as a conjecture to be investigated in further work.

One issue dominating all my discussion of isovist fields is the fact that these fields decompose into distinct types. These are based on the key elements of urban and architectural morphology which I casually suggest are long narrow elements like streets or corridors or halls, and smaller compact elements like squares or rooms. The various field maps reveal this but a clearer view is through the relationships between area and perimeter, and between area and the shape index $\{\Psi_i\}$. These are shown in the scatter plots in figure 4 where it appears that there are at least two types of isovist. These differences are also picked up when the frequency distributions of values in each isovist field are examined in figure 5 (over). As the T-shape is quite simple, and as there are no complex circumlocutions within the morphology, the average, minimum, and maximum distance distributions do not reveal any distinct types. These show mild negative and positive skews but when the area and perimeter distributions are examined, these distributions are trimodal with three distinct modal types. This is clearest in the distribution of areas. The largest are areas around the edge of the system where the vertical and horizontal extent of the T-shape can be seen, the smallest are above the T-shape where only one horizontal width can be seen, and the medium-sized are those which lie under each wing of the T-shape where most of a vertical side can be seen.

When we examine $\{\Gamma_i\}$, there is greater normality with only a mild positive skew. For the ratio $\{\Psi_i\}$, two modes are apparent, together with a long right-hand tail giving a highly positive skew. This reveals a small number of very compact shapes which lie between the inner corners of the T-shape, a larger number of less compact shapes
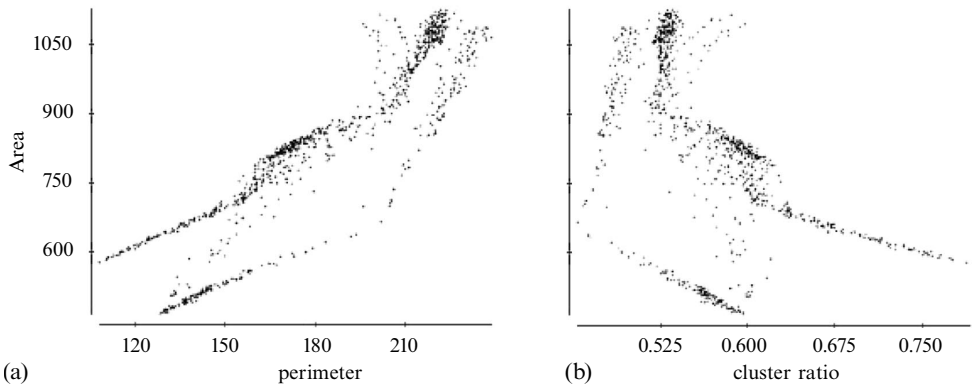
Figure 4. Scatter plots of isovists comprising isovist fields illustrating different varieties of isovist: (a) area against perimeter; and (b) area against the cluster-ratio $\{\Psi_i\}$.
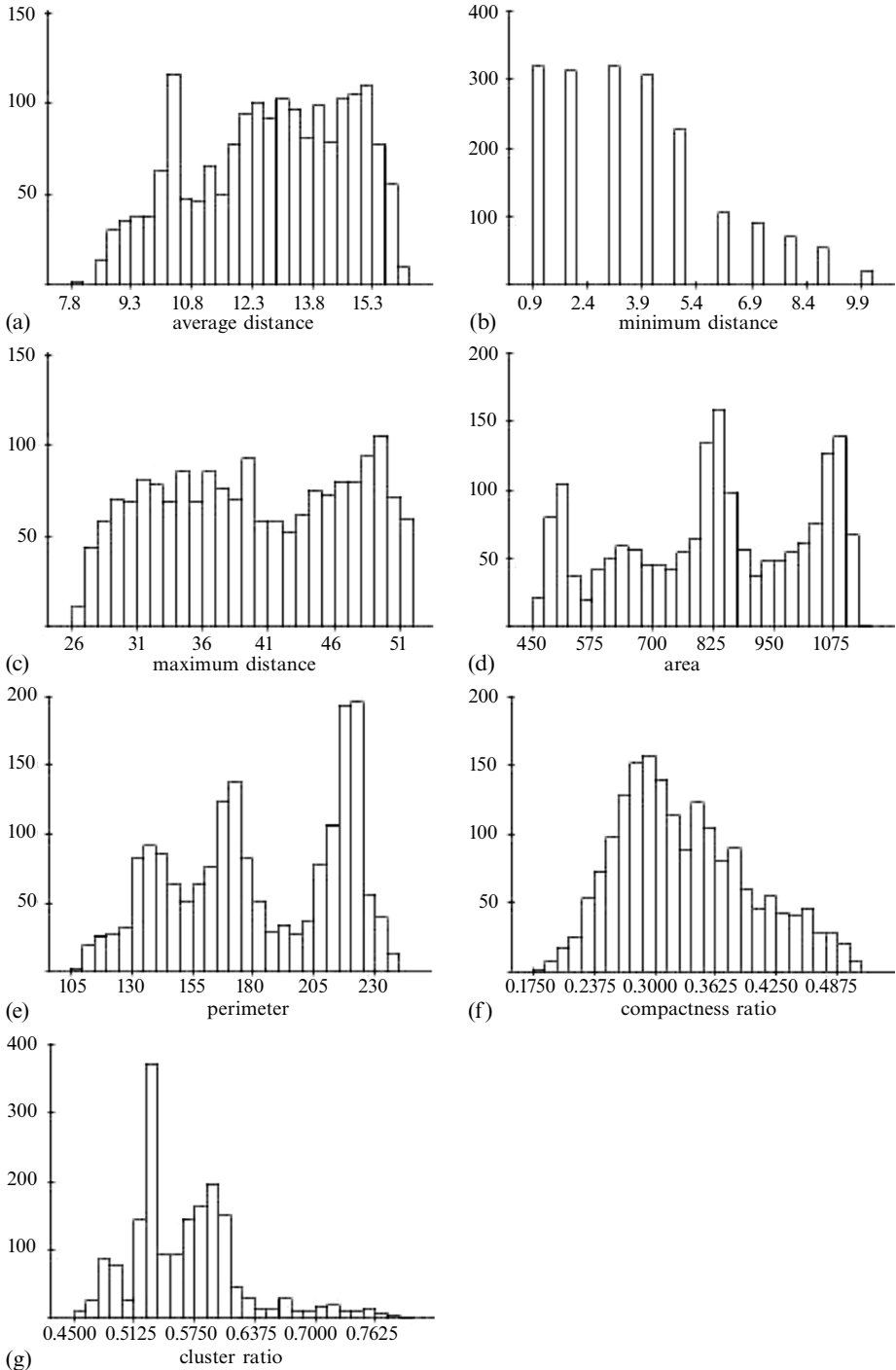
Figure 5. Frequency distributions of isovists comprising each isovist field: (a) average distance; (b) minimum distance; (c) maximum distance; (d) area; (e) perimeter; (f) compactness ratio; and (g) cluster ratio. The vertical axes are frequency counts in all cases, and in all subsequent similar graphs in figures 7, 9, 11, and 13.

Table 1. Properties and statistics of the isovist field: basic field data.

Application	Scale of vantage point: one square pixel	Size of pixel grid	Number of isovists (occupied pixels)	Percentage of grid occupied by isovists
T-shape	arbitrary	51×51	1840	0.707
Manhattan grid	arbitrary	133×133	1273	0.072
The Tate Gallery	1 m^2	187×187	9658	0.276
Regent Street	5 m^2	215×215	14667	0.317
Wolverhampton	36 m^2	187×187	6807	0.195

Table 2. Properties and statistics of the isovist field: compactness coefficient $\{\Gamma_i\}$.

| Application	Mean	Standard deviation	Skewness
T-shape	0.331	0.069	0.498
Manhattan grid	0.248	0.036	0.508
The Tate Gallery	0.235	0.102	0.596
Regent Street	0.181	0.107	0.712
Wolverhampton	0.164	0.065	0.839
A circle	1	–	–
A square	≈ 0.793	–	–
A straight line	0	–	–

Table 3. Properties and statistics of the isovist field: clustering/convexity coefficient $\{\Psi_i\}$.

Application	Mean	Standard deviation	Skewness
T-shape	0.567	0.059	1.080
Manhattan grid	0.234	0.027	−0.007
The Tate Gallery	0.443	0.113	0.235
Regent Street	0.378	0.092	0.445
Wolverhampton	0.488	0.102	0.454
A circle	1	–	–
A square	$0.866 \approx (\pi/2)^{1/2}$	–	–
A straight line	0	–	–

towards the edges, and a set of intermediate shapes between the corners of the square and the T-shape. There is a vast array of statistics which are routinely computed for these fields, but henceforth I will restrict my analysis to the two shape distributions which I 'loosely' refer to as the compactness index $\{\Gamma_i\}$ and the cluster or convexity index $\{\Psi_i\}$. For each of these, the mean, standard deviation, and skewness coefficients are listed. In tables 1–3, these values are shown for the basic T-shape, and for the second hypothetical example, the three real examples based on the Tate, Regent Street, and Wolverhampton, and some idealized morphologies based on regular geometries which provide benchmarks.

3.3 A more complex but regular geometry: the Manhattan grid

With the T-shape, the effects imposed by the outer boundary weight the edges in a way that distorts their influence. At the edge of the space, the area and the distance viewed may be a maximum, but the fact that there may be space beyond the edge lowers the average distance seen and distorts the indices of compactness and clustering. One can
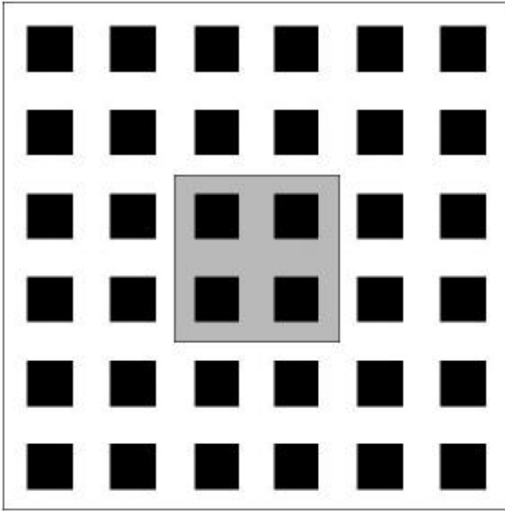
Figure 6. The inner and outer fields of the Manhattan grid.

easily remove this effect but it is preferable to do this using a regular repeatable shape. This can be done either by examining an inner field within a much larger field where the edge effects do not very much affect the inner field in question, or, in the case of StarLogo, by simply using the periodic boundary constraints—the wraparound features—which are part of the software. In fact, I will develop the analysis based on the former method, shown in figure 6. Note that the inner field is only one ninth the size of the overall field and that the farthest distance to be traversed is one third of the vertical or horizontal dimension of the overall space.

The inner field is made up of 4 square solid blocks in a wider field of 36, regularly spaced so that around 30% of the field is occupied by these blocks, leaving 70% empty. The inner field reflects these ratios, the analysis being based on a grid of 133×133 pixels. It seems intuitively obvious that the regular motif in figure 6 will generate equivalent regularity in the distributions across the isovist fields. In figure 7, we show six fields based on $\bar{d}_i$, $d_i^{\max}$, a_i, p_i, $\{\Gamma_i\}$, and $\{\Psi_i\}$ (excluding the minimum distance field now and hereafter) with the distribution of their field values in the associated histograms alongside. There is less to speculate upon with this morphology in comparison with the T-shape, in that our prior intuition is borne out. The fields decompose into two types: the spaces which are bounded by two solid blocks on either side which have lower distances, areas, perimeters, and shape ratios associated with them; and the spaces which are bounded by solid blocks on their four corners which, to all intents and purposes, have unrestricted views in the vertical and horizontal directions. The strongest correlations exist between average distance, area, and perimeter with all correlations being greater than 0.89. The compactness ratio is highly correlated with average distance but the clustering index shows much greater variation in being influenced by inner edge effects.

These two types of elemental shape are more clearly evident in the perimeter measures than in any relationships involving area. The scatter of average distances against perimeters shows two distinct sets of objects—inner square spaces between the edges of blocks and square spaces between the corners of blocks. This is less clear in the scatter against area, but when the frequency distributions are examined this bimodality of types becomes obvious. Average distance, maximum distance, and area are clearly bimodal in contrast to perimeter which is trimodal. The compactness
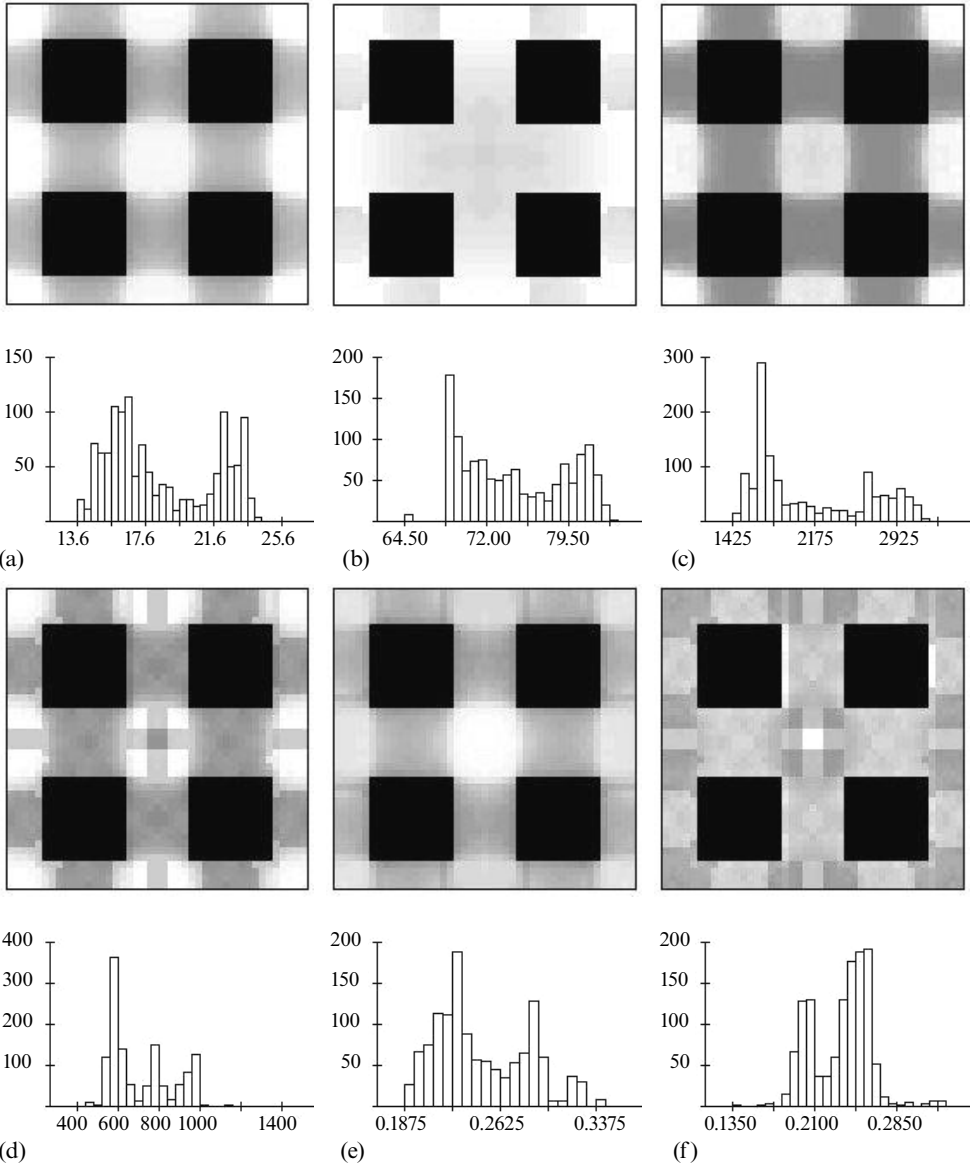
Figure 7. Isovist fields and frequency counts of isovists within their fields for the Manhattan grid: (a) average distance; (b) maximum distance; (c) area; (d) perimeter; (e) compactness ratio; and (f) cluster ratio.

and clustering indices are also bimodal, reflecting the two types of shape with the compactness distribution positively skewed, the clustering mildly negative, notwithstanding its long right-hand tail. In tables 1–3, moments of these distributions are shown and this immediately reveals what visual intuition suggests: that the isovists associated with the Manhattan grid are much less compact and clustered than their T-shape equivalents.

4 Applications: building and street morphologies at different scales

4.1 A complex building: the Tate Gallery

Isovist analysis to date has been restricted mainly to house plans associated with famous architects, although some of these have been quite complex in terms of the way shapes are juxtaposed (Benedikt, 1979). In suggesting the need for an extensive classification of examples prior to the development of proper theory, my focus is upon the more mundane where dramatic viewpoints and perspectives, insofar as they exist at all, have not been the main criterion for selection. Here we will begin with a 19th-century neoclassical building, London's Tate Gallery, which is composed of many rooms linked by narrow, tiny halls which pan out into wider galleries. Insofar as the building can be said to be complex, this occurs from its juxtaposition of long vistas with short vistas, but in this sense it is not very different from a streetscape assembled from various types of square or piazza. The room plan is shown in figure 8. Note that Turner et al (2001) use a version of the Tate which includes the new Clore Extension attached to the lower right-hand section of the Gallery and thus my results cannot be compared directly with theirs.

The number of isovists within the Tate is much higher than in the two theoretical examples that have been dealt with so far. The space is represented by 9658 grid points, and is composed of around 50 rooms linked by openings in walls and by short vestibules. In this example, it is difficult to detect the basic elements of space, although it is likely that there are distinct differences between long axial views and shorter, more compact spaces which reflect the structure of the gallery. In figure 9, the six isovist fields with their frequency distributions are illustrated. There are clear spatial correlates between each of the fields based on the domination of a few long axial lines which define the overall linear structure of the gallery. This is less clear for average distance but it is very marked for maximum distance, area, and perimeter which are all highly correlated.

The index of compactness behaves as we might anticipate. Typical vistas within the gallery cut across and through quite compact rooms, thus marking out lines of sight rather clearly, and tending to emphasize the fact that the most compact spaces are the smaller, squarer, and more remote rooms in the gallery. The index of clustering also correlates with compactness at 0.662, but what is very clear is that the spatial patterns manifest in these fields are not detected at all well by these statistics. In short, there
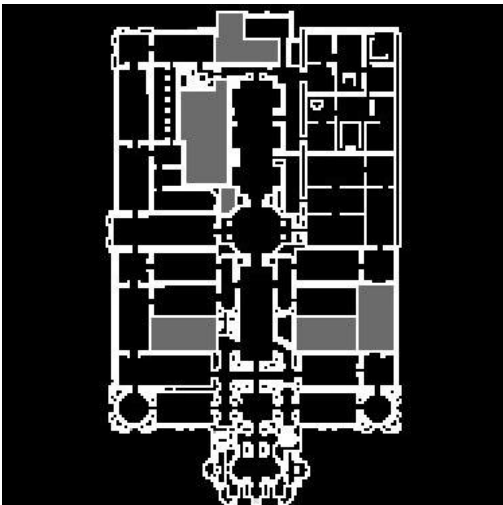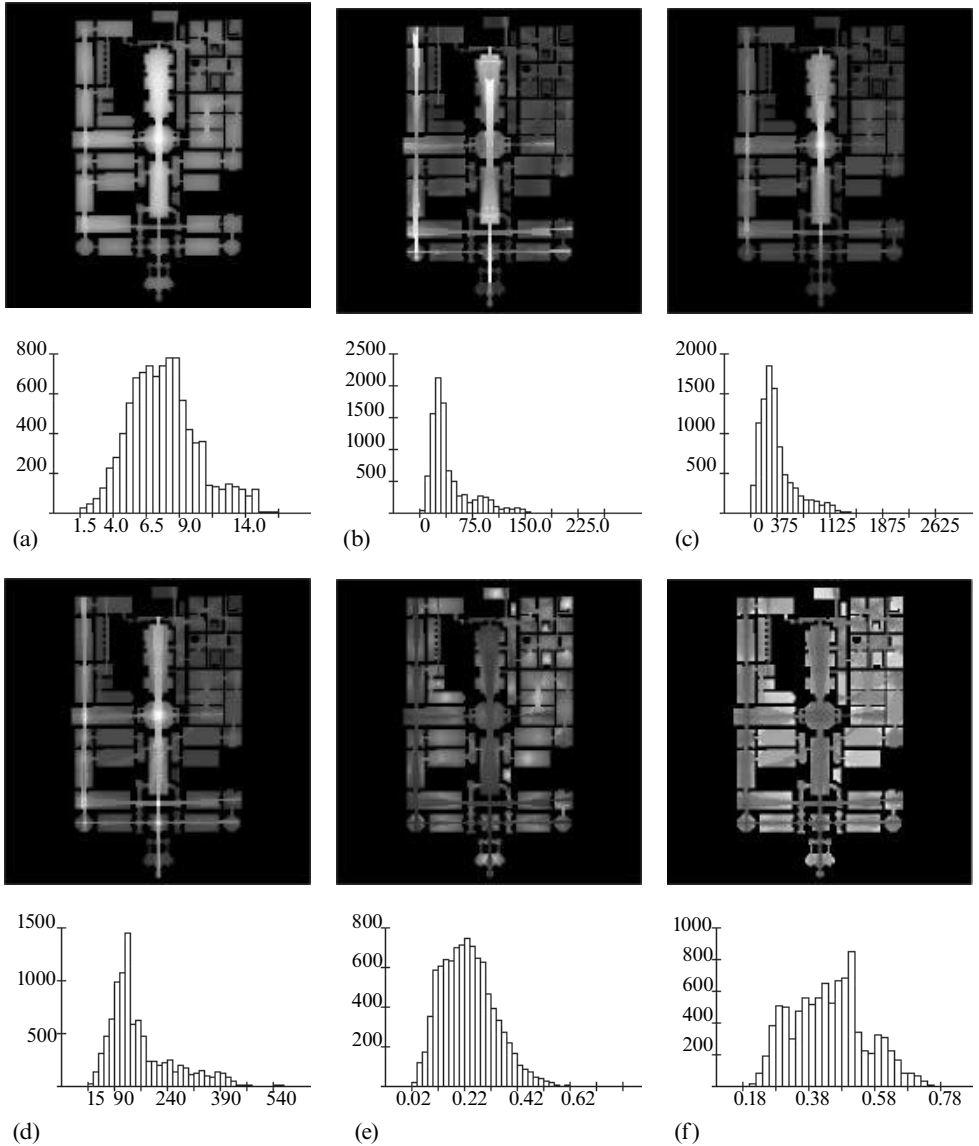

Figure 8. Room plan for the Tate Gallery, excluding the Clore Extension.

Figure 9. Isovist fields and frequency counts for the Tate Gallery: (a) average distance; (b) maximum distance; (c) area; (d) perimeter; (e) compactness ratio; and (f) cluster ratio.

is substantial 'spatial correlation' between various fields which is not picked up in the actual correlations, although a cursory comparison of the field maps in figure 9 immediately reveals such correlates. The fact that such patterns cannot really be detected statistically is also revealed in the scatter graphs which can be plotted between any pair of the six fields. It is not possible to break these into separate scatters as was possible in the previous examples. In short, the patterns that we see in the Tate's isovist fields—fan-like vistas everywhere—are not reflected in a simple set of distinct morphological elements.

The frequency distributions simply confirm what we have already implied. All the distributions are positively skewed, particularly the maximum distance, area, and perimeter distributions. None of the histograms shows any degree of bimodality,

once again reinforcing the notion that the Tate is a constellation of vista types rather than different types of geometric spaces. However, it is also clear from tables 1 – 3 that, although the compactness index for the whole system is lower than in the first two examples, the cluster index is a lot higher than for the Manhattan grid, meaning that spaces are well connected even though they may be somewhat less compact. This example has shown that, once we move to real examples, bimodalities in the distribution of isovists with their fields may not exist, thus implying simpler patterns. But, in another sense, the spatial patterns are more complex; spatial objects which are not physically distinct but distinct only in terms of the patterning of the visual field, take on greater significance.

4.2 Streets and squares: Regent Street and Piccadilly Circus

The next example is the most intricate and certainly the largest. The spaces in the constellation of streets and squares in London's Regent Street area can be represented by the 14 667 grid points shown in figure 10. This area of central London comprises a mixture of planned and incremental development. Regent Street and Regent's Park to the north were laid out in the early 19th century by the classical architect John Nash, the street itself being one of the most important Georgian town plans of that period. The area in figure 10 begins halfway down Regent Street, and takes in the curve into the somewhat irregularly shaped piazza of Piccadilly Circus. Most of the area, however, comprises the streets in the backland to the east of Regent Street and north of Piccadilly Circus. Here there is a regularly proportioned square—Golden Square—into and across which flow long narrower streets, bounded by shorter ones such as Carnaby Street, which merge into Soho. One of the obvious characteristics of this morphology is its composition as a set of rather distinct, long streets with a smaller number of squares of different shapes.

Figure 10. Regent Street and Piccadilly Circus.

The six isovist fields are shown in figure 11 where the effect of these long streets is immediately clear. The maps of average distance and area are highly correlated at 0.942 and fairly smooth in their spatial variation. Their smoothness is slightly interrupted by the long, narrow streets which cut into squares and across wider streets. This is revealed in the map of maximum distances where the effect of the massive curve in Regent Street is evident in the way this interferes with vistas. This distance map is
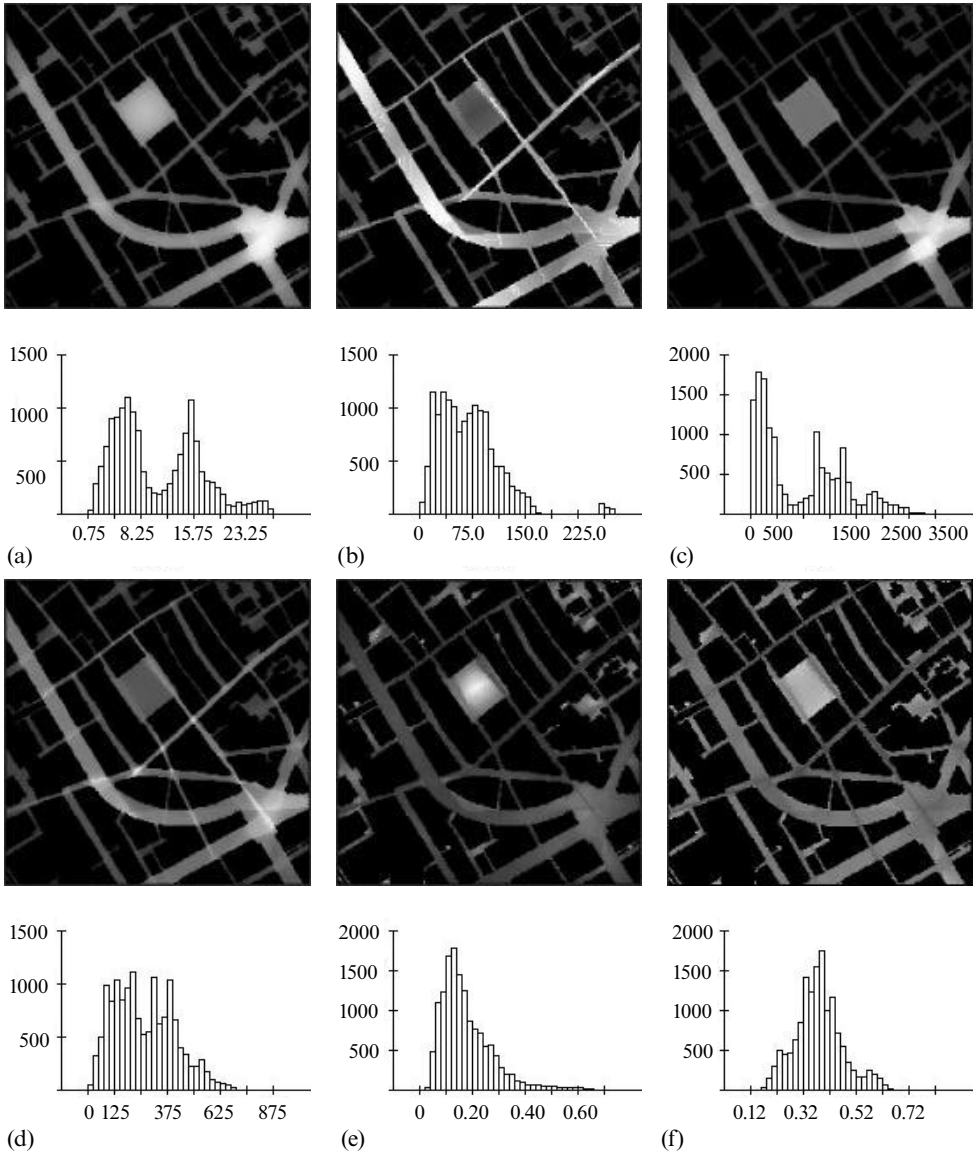
Figure 11. Isovist fields and frequency counts for Regent Street: (a) average distance; (b) maximum distance; (c) area; (d) perimeter; (e) compactness ratio; and (f) cluster ratio.

quite highly correlated with perimeter at 0.784, whereas the area and perimeter maps are highly correlated with each other in the same manner as average distance and area. The two space indices pick up these effects in different ways. The compactness index is dominated by Golden Square, whose central vantage point is the most compact of anywhere in the area; the tiny squares, which are simply indentations in the street system, are more compact than the long narrow streets which tend to dominate the entire morphology. The index of clustering shows up these patterns quite clearly, with the long streets having low convexity values in contrast to squares which have much greater convexity in shape. This can be seen in Golden Square and in Piccadilly Circus where streets cut across these squares, defining nonphysical geometries—visual fans which indicate variety in the spatial experiences gained from moving within these places.

The correlations between the six fields have the same pattern as in all previous examples with area, average distance, and perimeter being the most closely related. The scatter graphs formed from any pair of these distributions do not show particularly clear differences between the long streets and more compact vistas within squares but, when the frequency distributions are examined (also in figure 11), these differences are marked. The distributions of average distance, area, and perimeter are clearly bimodal with mild positive skews, reflecting features of the morphology already discussed. The farthest distance field is very positively skewed with a long right-hand tail associated with the few very long streets within the morphology. These streets and their isovists, although small in number, are significant in their effect. When the shape fields are examined, the compactness index is again positively skewed, reflecting the fact that there are only a small number of very compact objects in the scene. The convexity index, however, is much more normally distributed. In both of these cases, the bimodality of the basic measures cancels itself out, revealing that the visual objects which constitute the scene are reasonably distinct with respect to all the basic measures.

From the indices presented in tables 1 – 3, the compactness index is the lowest in all our examples to date, reflecting the domination of long streets. The convexity average is a little less than that of the Tate but not as low as that of the Manhattan grid. What is particularly clear again in this example, is that the actual physical morphology of such complex urban building and streetscapes cannot best be measured by the geometry itself but is more likely to be represented by the visual 'objects' or spaces which emerge as a result of this geometry. Our next example reinforces this point.

4.3 An entire town centre: Wolverhampton

Wolverhampton is a town in the UK Midlands which is one of the very few whose commercial and retail core is bounded by a complete ring road constructed during the last 30 years. As the industrial town grew up from the early 19th century on, the pattern of streets within it has evolved from the original main street along the highway from Birmingham to the northwest, to a more compact center around this original seed. Wolverhampton does not have any classic squares or streetscapes in the manner of London's West End, but there is a spacious civic center in Queen Square and St Peter's Square, and a covered shopping center—the Mander Centre—which is an early in-town mall. The morphology is thus composed largely of streets and, although these are as

Figure 12. Street plan for Wolverhampton town center.

long and as narrow as those in the Regent Street area, the scale at which these are presented makes them a little shorter than those in our previous example. The town center is shown in figure 12.

The isovist fields are mapped in figure 13 from which it is clear that streets dominate the scenes. The average distance from each vantage point simply mirrors the fact that there is more space at junctions of streets and in the occasional interstices that feature in the street scenes as a result of random redevelopment and vacant plots. As in previous examples, this field is the smoothest of all, being composed of averages in contrast to the maximum distance which is dominated by four or five long streets. However, the fact that geometrically you can see for a long distance is often a result of the juxtaposition of streets which take no account of any other visual intrusions or
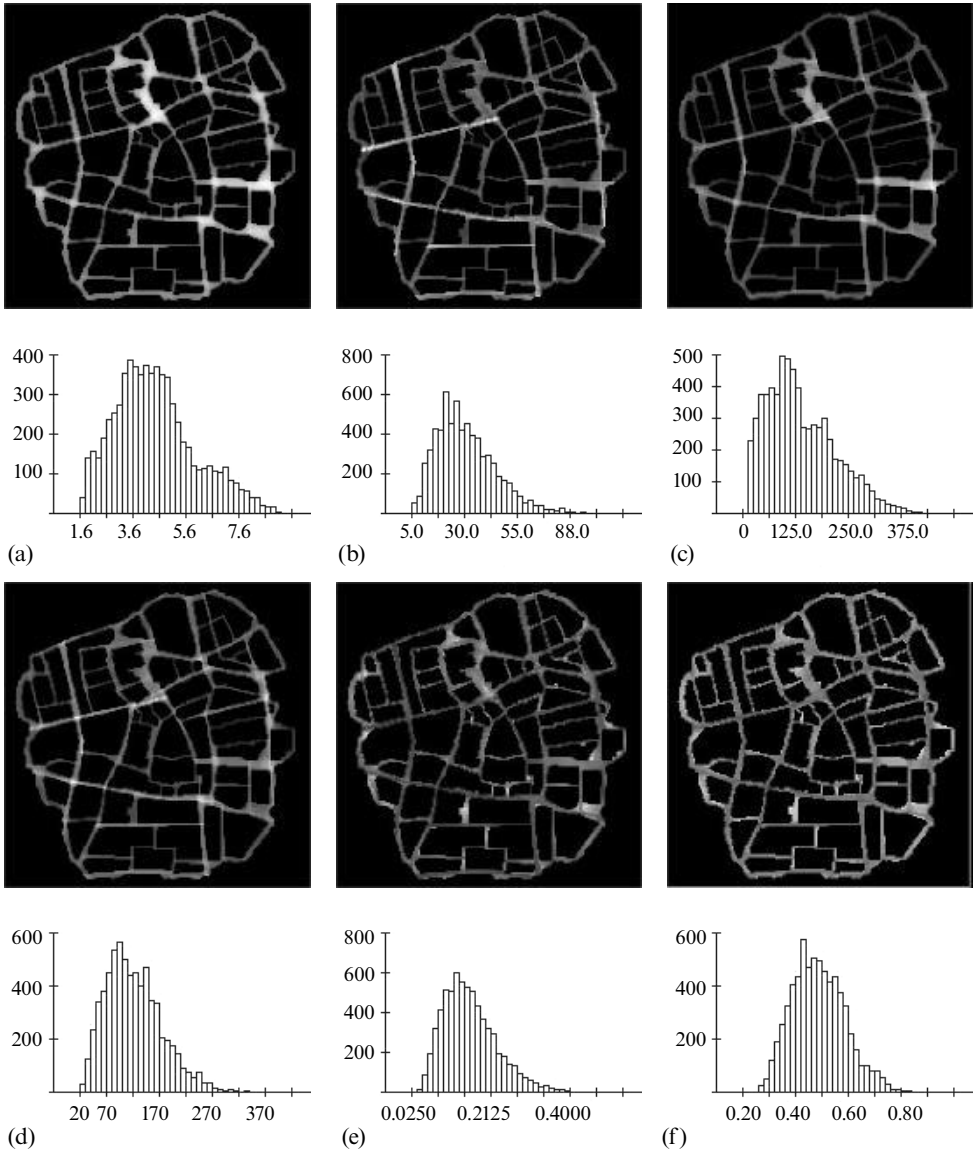
Figure 13. Isovist fields and frequency counts for Wolverhampton center: (a) average distance; (b) maximum distance; (c) area; (d) perimeter; (e) compactness ratio; and (f) cluster ratio.

features that draw attention away. In this sense, we should perhaps be working at a much finer level of resolution so that we can pick up visual disruptions caused by such obstacles. This supports the point implicit in the quote cited earlier from Peponis et al (1997) who caution that isovist analysis is potentially limited by the scale of resolution. The area and perimeter fields detect the interaction between squares and streets a little more clearly; these fields show that areas and perimeters where streets enter squares have the largest values. The average distance, area, and perimeter fields are highly correlated with one another with correlations greater than 0.75 in every case, similar to all the other examples in this paper.

The compactness and convexity measures do not reveal any surprising features. The inner parts of squares and some junctions have the highest compactness with the middle portions of long streets having the least. The convexity field shows that areas on the edges of streets have higher convexity than the center lines, this being a result of the relative irregularity of the town plan. Unlike previous examples, it is not possible to detect distinct elements in the visual fields of Wolverhampton town center. The street scenes appear to be relatively uniform. If the scatter plots between any pair of the six distributions are examined, there are no clear groupings. This is further reinforced by the frequency plots, also shown in figure 13 where there is no evidence whatsoever of any bimodality or other major deviations from normality. All six plots are positively skewed but only mildly so, with the exception of the convexity index which is almost normally distributed. The moments for the shape indices are presented in tables 1 – 3 from which it is clear that Wolverhampton has the lowest average compactness of any of the examples we have dealt with, a fact that simply confirms a morphology dominated by long streets.

5 Summarizing space: morphological covers and signatures
5.1 Covering space using ranked isovists
So far, I have dealt with rather basic properties of isovists. However, in research on urban and architectural morphology to date, there has been a concern to use such properties to identify larger spatial units that compose a scene and give it integrity of some kind.

This is the motivation behind space syntax which orders streets on the basis of their relative accessibilities (Hillier and Hanson, 1984), and behind the convexity analysis being developed by Peponis et al (1997). Indeed questions such as 'what is the minimum number of isovists (vantage points) from which an entire environment can be seen' were explicitly posed by Benedikt (1979) in his initial exposition, and by Davis and Benedikt (1979) in their more technical presentation. Such extensions take us in a very different direction and all we can do here is indicate how we might proceed. It may even be argued that, once isovist fields have been computed, the raw information that they provide is often enough for the kind of analysis that morphologists have hitherto required. Nevertheless, by way of conclusion, we will explore two problems involving the interpretation of isovists: first the 'covering problem' which involves finding a unique set of isovists which cover the entire space; and second the 'signature problem' which involves examining the flow of information associated with any particular path through the isovist field.

The problem of decomposing or partitioning a complex space into a small number of relatively distinct pieces can be seen as equivalent to that of aggregating the points that define a set into subsets that meet some similar criterion. This type of problem can also be framed as one of finding a set of points which cover the space. If the criterion is that the entire space must be visible from these points, this is akin to finding a set of isovists which cover the space or cover the perimeter of the space, problems which are

usually coincident. This latter problem was posed over 20 years ago in computational geometry as the 'art gallery problem'. It is defined as selecting a number of 'guards' who can see all the 'pictures' in the gallery which is the same as defining a number of vantage points from which the entire gallery can be seen. For any polygon with P vertices or edges, a simple theorem exists which shows that, at most, $P/3$ guards or isovists are sufficient and sometimes necessary to cover the space; if the space has H holes, then $(P + 2H)/3$ guards are required (O'Rourke, 1987). This number is a maximum; for most cases, it is a lot less, and for the case of a convex polygon, it is just one. However, the problem of choosing a minimum number of isovists for any polygon is intractable for it is NP (not-in-polynomial time)-hard (O'Rourke, 1987). This is perhaps a little disappointing for space syntax theorists as it implies that there is no unique minimal set of convex partitions which partition space and thus no unique set of axial lines. However all is not lost. As Peponis et al (1997) demonstrate, there still exist simple algorithms for partitioning space into a small number of convex sets which make space intelligible.

It is easy to see why convexity is relevant, because if a unique decomposition into convex sets is possible, then this immediately provides a unique set of points that cover the space. However, I will proceed by defining a unique set of isovists which may be overlapping but which still cover the space. In essence, I rank the isovists in a field with respect to a given criterion—in this case, how much area $\{a_i\}$ can be seen from each vantage point i—then I select isovists from this ranking, starting with the largest area seen and then choosing isovists which are not within the neighborhoods of any isovists chosen so far (but may overlap them), continuing until the entire space has been exhausted. Formally, I first choose the isovist $k = \max_i\{a_i\}$ from the set of all isovists—the isovist field Z—and then form the next set of isovists $i \in \{Z - Z_k\}$, and choose another isovist $l = \max_i\{a_i\}$ from this new set; the process continues with the reduced set $\{Z - Z_k - Z_l\}$ until the space is exhausted. Although it cannot be proved that the number of isovists that cover the space is less than $P/3$ [or $(P + 2H)/3$ if the space has holes], one intuitively 'knows' that this is likely to be so because of the continuity and regularity of space. I will now illustrate this for the Tate Gallery.

By using the art gallery theorem, where the Tate shown in figure 8 has $P = 820$ edges and $H = 33$ holes, there are, at most, 296 isovists which cover the space. By using our algorithm, the gallery can in fact be covered by 84 isovists, the first three of which are shown in figure 14. In figure 15(a) (over), I show the 84 points defining these isovists; in figure 15(b), the actual isovists, with the first shown as the top layer, the second one below, and so on; in figure 15(c), the number of overlaps of isovists,

(a)   (b)   (c)
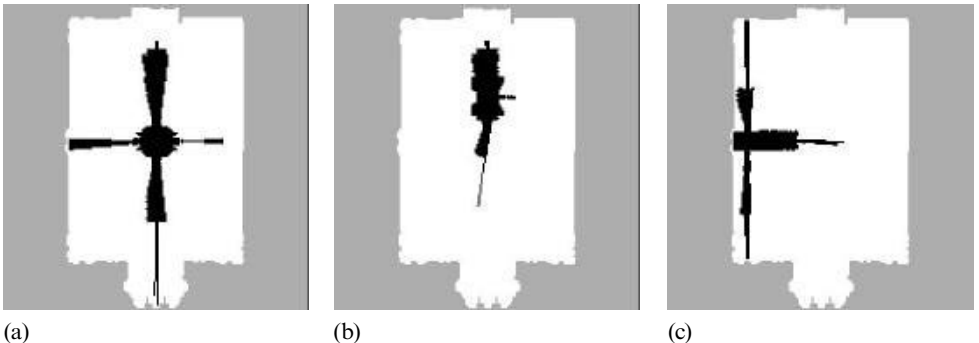
Figure 14. The top three isovists, ranked from (a) to (c) by area viewed, with independent origins.

(a)

(b)

(c)

(d)
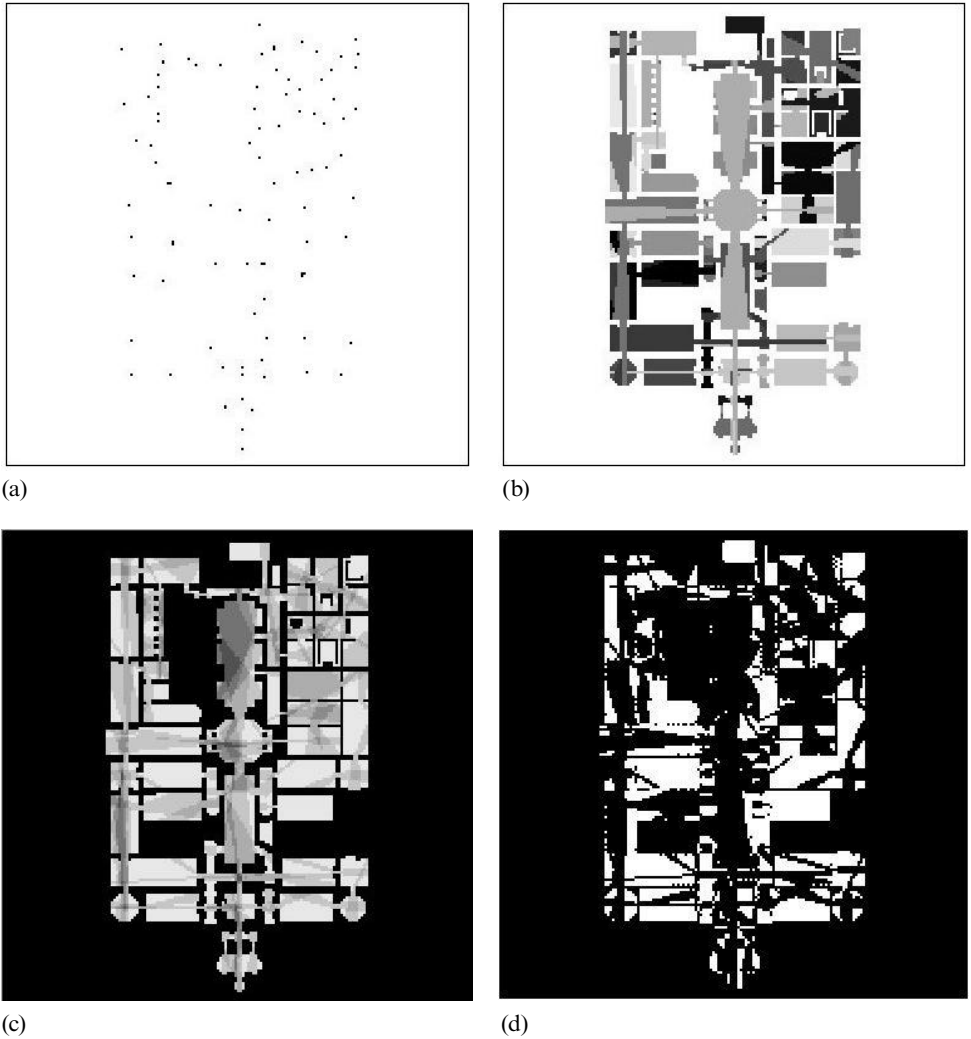
Figure 15. The isovist cover: (a) the 84 isovist points; (b) the ranked isovists in layers; (c) the number of isovist overlaps; and (d) the areas covered by single isovists.

with the darker shading indicating more overlaps; and in figure 15(d), the areas of the gallery which are covered only by a single isovist. Although this is a unique partition, it is not necessarily the minimum number of isovists. It might be taken as the starting point in a more comprehensive algorithm, in which an isovist must be swapped for another each time a new isovist covers more than a certain percentage of one (or all) already chosen. The percentage threshold of cover can then be gradually relaxed until the entire space is covered. Simulated annealing or the genetic algorithm might be used to occasion the swaps. For example, in figure 14, the second isovist chosen covers the first by 75%. If this were not allowed, and the third were chosen instead, then the ultimate distribution and number of isovists would be different. There are endless variations of this kind that might be tried.

5.2 Morphological signatures

One of Benedikt's (1979) motivations for introducing isovist analysis was to record "a sudden rush of information—a sudden dilation of [his] view and exposure too"

(page 58), posed by traveling along a path within an isovist field. Benedikt and Burnham (1985) also demonstrated the coincidence of this analysis for measuring actual perceptions in an experimental context. Conroy (2000) has taken this idea much further by associating such changes in perception with characteristics of isovist fields and the detailed geometric character of streets and their intersections, albeit in virtual rather than real environments. It is also easy to simulate this kind of experience in StarLogo. This first involves tracing out a path within the isovist field, placing an agent at a starting point on the path, and programming the agent to follow the path from start to finish. At each step on the path, the agent captures information from the isovist fields which have already been computed by the original program. This information provides the set of signatures describing the spatial experience of walking the path, and is best represented as a profile along the path.

An interesting path through Regent Street is shown in figure 16. Starting a little way down the northern end of the street (south of Oxford Circus) the path doglegs northeast into Carnaby Street and turns southeast through Golden Square and thence into Piccadilly where the walker circumnavigates the Circus before turning west into Regent Street again. To avoid the curve of Regent Street, the path turns north and then west into Glasshouse Street, which enters Regent Street once again at the end of its curve, turning back towards the northwest and its start point. A casual comparison of the path in figure 16 with the six isovist fields in figure 11, indicates that a variety of spatial experiences in terms of the urban geometry are captured on this walk: ranging from long views along narrow streets, to complex views within squares, to much more open sensations which occur in the wider streets and spaces.
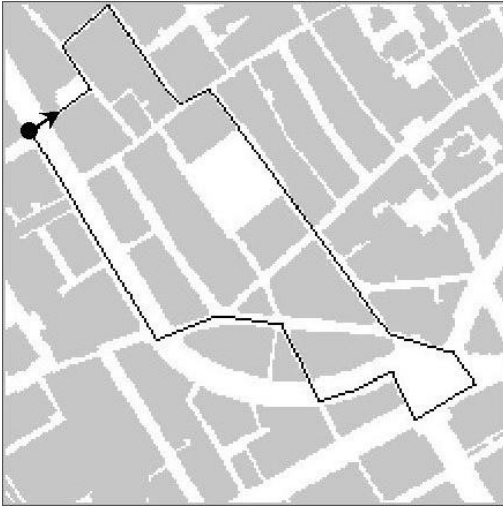
Figure 16. An interesting path through the Regent Street area.

The path is 581 pixels in length. The profiles of the six measures along this length are shown in figure 17 (see over). Total area seen from this path is correlated very strongly with the average distance seen and these profiles, in figures 17(a) and 17(c), illustrate clearly the changes in space encountered as the walker moves from streets to squares. In fact, the walk is dominated by narrow streets where the walker can see a long way, except when entering Regent Street from Piccadilly Circus where the curve obstructs vision and in the upper part of the street where the edge effects lessen actual distance seen. What is of interest is the fact that there are some positions—for example, in Piccadilly Circus—where the walker can see long distances and large
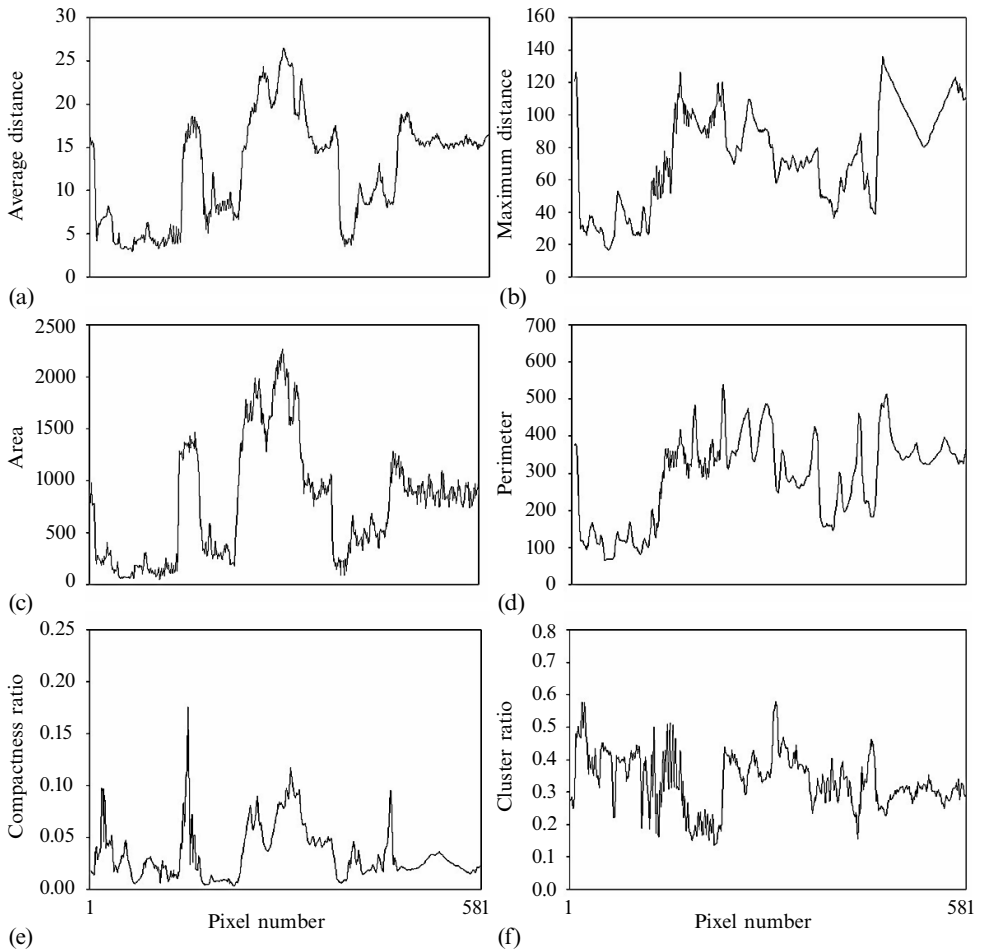
Figure 17. Traces across isovist fields formed by the walk through Regent Street for: (a) average distance; (b) maximum distance; (c) area; (d) perimeter; (e) compactness ratio; and (f) cluster ratio.

areas, thus providing a measure of spaciousness, a 'true' sensation of what a real walker might feel in this area. This feature of the walk is also picked up from the perimeter measure which increases quite dramatically at major junctions. The index of compactness, however, which captures how enclosed the walker feels, is very sensitive to changes in both direction and the area seen, whereas the clustering or convexity of spaces defining the walk is more uniform as a trend, yet much more 'noisy' as a profile in that this measure picks up all the local detail associated with the pixelation of the street map. These profiles should be manually traced out in the walk in figure 16.

6 Conclusions: directions for future research

Twenty years after Benedikt's (1979) ground-breaking work, I have demonstrated that it is now routinely possible to compute isovist fields, to display them in standard ways, and to develop basic statistical measures which detect explicable and meaningful variations in architectural and urban morphology. A start has been made on classifying different types of morphologies, although it is clear that a much wider range of types will be required before the rudiments of any theory of morphology can be

fashioned around these ideas. In this paper I have raised many more questions than I have sought to answer and, in conclusion, I will identify six different areas which appear promising and urgent if these ideas are to be further developed.

First, it is still necessary to develop better measures of shape which are consistent with new ideas concerning convexity inspired by Peponis et al (1997; 1998a; 1998b) and Turner et al (2001), as well as isovist geometry developed by Conroy (2000). The idea of embedding visibility graphs into more conventional representations of Euclidean space, moving from one to another perhaps in the manner suggested by Watts (1999), appears promising. Second, this analysis reveals that the morphologies associated with buildings and street systems in cities provide a set of spatial experiences which reflect a subtle mixture of the hard physical geometry of space with moving viewsheds which, in turn, have their own geometry. For example, in several of the examples, compact open spaces with their own physical homogeneity are subtly partitioned into local fields which depend upon observers moving linearly through streets or corridors that connect these spaces into the wider physical fabric. These elements are hard to detect by using conventional statistics and this suggests that a specific statistical theory must be developed for such problems if the interplay of geometry and the local dynamics of visual movement are to be thoroughly understood.

Third, I have barely broached the issue of scale, but it is clear that the measures are not scale invariant, that the visual experiences as detected by these measures will vary across scale, and that local detail at very fine levels may interact with my interpretations in ways that it is not yet possible to simulate. For example, other moving observers in the field or viewshed, as well as small but significant fixed obstacles to movement, may change the geometrical measurement of isovist fields in ways that can be handled only by using levels of resolution well beyond our current capabilities (Peponis et al, 1997). Fourth, although I am conscious of boundary effects and the idea that fields are constrained by boundaries, much larger systems are required, within which the specific focus of interest is embedded in a way that minimizes such effects. This was the way in which the Manhattan grid example proceeded, but in Regent Street, it was not possible to extend the system to take account of lines of sight outside the system, which in this case has probably produced significant distortions in the visual fields.

Fifth, there are a variety of partition problems that involve summarizing isovist fields in ways that simplify space into distinct subspaces or covers. In one sense, this has been the traditional way in which morphologies have been represented, as in space syntax analysis, but the great attraction of representing space as isovists is that basic morphological data are preserved prior to any such simplification taking place. Finally, the influence of isovist theory in design must be noted. Although the theory is still rather primitive in terms of its use in interpreting spatial experiences, it can and should be used for evaluating experiences in proposed, as well as existing, morphologies. Evaluating new and radical spatial configurations is but another test and extension of this approach.

References
Batty M, Jiang B, 2000, "Multi-agent simulation: computational space – time dynamics in GIS", in *Innovations in GIS VII: GIS and Geocomputation* Eds P Atkinson, D Martin (Taylor and Francis, London) pp 55 – 71
Benedikt M L, 1979, "To take hold of space: isovists and isovist fields" *Environment and Planning B* **6** 47 – 65
Benedikt M L, Burnham C A, 1985, "Perceiving architectural space: from optic rays to isovists", in *Persistence and Change* Eds W H Warren, R E Shaw (Lawrence Erlbaum, Hillsdale, NJ) pp 103 – 114
Buckley F, Harary F, 1990 *Distance in Graphs* (Addison-Wesley, Reading, MA)
Conroy R, 2000 *Spatial Navigation in Immersive Virtual Environments* unpublished PhD thesis, University College London, Gower Street, London WC1E 6BT
Davis L S, Benedikt M L, 1979, "Computational models of space: isovists and isovist fields" *Computer Graphics and Image Processing* **11** 49 – 72
Hillier B, Hanson J, 1984 *The Social Logic of Space* (Cambridge University Press, Cambridge)
O'Rourke J, 1987 *Art Gallery Theorems and Algorithms* (Oxford University Press, New York)
Peponis J, Wineman J, Rashid M, Kim S H, Bafna S, 1997, "On the description of shape and spatial configuration inside buildings: convex partitions and their local properties" *Environment and Planning B: Planning and Design* **24** 761 – 781
Peponis J, Wineman J, Bafna S, Rashid M, Kim S H, 1998a, "On the generation of linear representations of spatial configuration" *Environment and Planning B: Planning and Design* **25** 559 – 576
Peponis J, Wineman J, Bafna S, Rashid M, Kim S H, 1998b, "Describing plan configuration according to the covisibility of surfaces" *Environment and Planning B: Planning and Design* **25** 693 – 708
Ratti C, Richens P, forthcoming, "Urban texture analysis with image processing" *Environment and Planning B: Planning and Design*
Resnick M, 1994 *Turtles, Termites, and Traffic Jams* (MIT Press, Cambridge, MA)
Turner A, Doxa M, O'Sullivan D, Penn A, 2001, "From isovists to visibility graphs: a methodology for the analysis of architectural space" *Environment and Planning B: Planning and Design* **28** 103 – 122
Watts D J, 1999 *Small Worlds: The Dynamics of Networks between Order and Randomness* (Princeton University Press, Princeton, NJ)
Watts D J, Strogatz S H, 1998, "Collective dynamics of 'small-world' networks" *Nature* **393** 4 June, 440 – 442